

Alternatives to the CO Ligand: Coordination of the Isolobal Analogues BF, BNH₂, BN(CH₃)₂, and BO⁻ in Mono- and Binuclear First-Row Transition Metal Complexes

Andreas W. Ehlers, Evert Jan Baerends,* F. Matthias Bickelhaupt, and Udo Radius

Abstract: Transition metal complexes containing boron ligands (BE) coordinating through boron are viable targets for synthetic chemistry. This follows from our density-functional theoretical investigation of the metal-binding capabilities of a series of isolobal ligands AE (CO, BF, BNH₂, BN(CH₃)₂, and BO⁻) in mono- and binuclear first-row transition metal carbonyl complexes [M(CO)_n(AE)], [Fe₂(CO)₈(AE)], and [Mn₂(Cp)₂(CO)₄(AE)] (M = Cr–Ni). A detailed analysis of the M(CO)_n–BE bond shows that BE ligands are much better σ donors than CO and comparable π acceptors (except for

BO⁻, which is a poor π acceptor owing to its high energy π^* LUMO). The M(CO)_n–BE bond is therefore significantly stronger than the M(CO)_n–CO bond. The [Cr(CO)₅(AE)] bond dissociation energy, for example, amounts to 41.8 (CO), 62.1 (BF), 72.1 (BNH₂), and 93.4 kcal mol⁻¹ (BO⁻). However, the high polarity of the BE ligands and the build-

up of positive charge on BE suggest a low kinetic stability. Strategies for improving the kinetic stability of metal–BE complexes are presented. Steric protection of the reactive BE frontier orbitals may be built into the ligand as in BNR₂ (with R potentially bulky) and into the metal fragment (by bulky ligands or μ coordination). However, the electronic stabilization of the [M]–BE bond seems to be just as important. We show that binuclear metal complex fragments, such as Fe₂(CO)₈ and Mn₂(Cp)₂(CO)₄, have just the right frontier orbitals to accomplish this.

Keywords: boron • isolobal relationships • orbital interactions • theoretical calculations • transition metals

Introduction

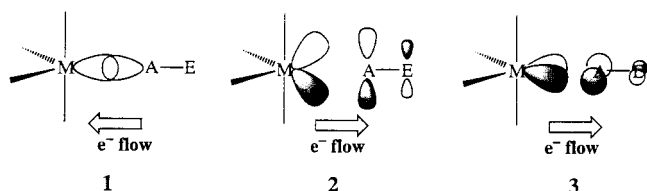
Transition metal carbonyl complexes constitute one of the most important families in organometallic chemistry, displaying a wealth of structural complexity and chemical reactivity. They are also of great practical importance as starting materials for the synthesis of other low-valent metal complexes or as reagents in organic synthesis (e.g. Collman's reagent, Na₂[Fe(CO)₄]).^[1,2] They also play a key role as intermediates in homogeneous catalysis.^[3] The possibility of substituting CO by a large number of other ligands contributes to the rich diversity. Examples for such ligands are halides (X⁻), alkoxides (RO⁻), phosphines (PR₃), or aromatic

rings (C₆H₆, C₅H₅⁻). Ligands isolobal to CO (for example N₂, NO⁺, and CN⁻) are also quite well-known. However, the number of complexes with neutral isolobal molecules terminally ligated to transition metals is somewhat limited; they are mainly complexes with carbon ligands of the type CE (E = S, Se, Te, NR, CH₂) and with N₂. None of these ligands seems to be as versatile as CO.

It would be very useful to have at one's disposal an assortment of ligands that are similar to CO and yet different. One could use these to fine-tune the activity of transition metal based catalysts and thus improve the efficiency of catalytic processes. Recently, we have undertaken a theoretical exploration of practical alternatives to the ubiquitous and immensely useful CO ligand.^[4] A careful comparative analysis of the isoelectronic diatomics AE (N₂, CO, BF, and SiO) and their metal-binding capabilities in the model complexes [Fe(CO)₄(AE)] and homoleptic [Fe(AE)₅] has underlined that for the formation of stable metal-ligand bonds it is essential to have good and balanced σ donation through the 5 σ orbital (Scheme 1, **1**), and π acceptance through the 2 π orbitals (Scheme 1, **2** and **3**).

CO has just the right orbital electronic structure to provide such balanced, synergic bonding: a moderately high-energy 5 σ HOMO, largely localized on carbon and directed towards the metal center, and moderately low-energy 2 π LUMOs, again

[*] E. J. Baerends, A. W. Ehlers
Afdeling Theoretische Chemie
Scheikundig Laboratorium der Vrije Universiteit
De Boelelaan 1083, NL-1081 HV Amsterdam (The Netherlands)
Fax: Int. code + (31) 20444-7643
e-mail: baerends@chem.vu.nl
F. M. Bickelhaupt
Fachbereich Chemie, Philipps Universität Marburg
Hans Meerweinstrasse, D-35032 Marburg (Germany)
U. Radius
Institut für Anorganische Chemie
Universität Karlsruhe, Engesserstrasse Geb. 30.45
D-76128 Karlsruhe (Germany)



Scheme 1. Orbital diagrams showing σ donation and π acceptance of AE ligands.

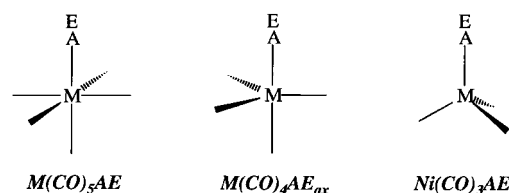
localized to a large extent on carbon. Together with substantial intrinsic stability, this is of course what makes the CO ligand so versatile. Some of these features, so important for the stability of the M–AE bond, were found to be even more pronounced in the electronic structure of other ligands.^[5] The 5σ orbitals are at higher energy and the $2\pi^*$ are at lower energy in SiO and BF. In BF these frontier orbitals are also more strongly localized on the A atom (i.e. boron). Indeed the polar BF is found to bind even better to first-row transition metal centers than CO especially because of its excellent σ -donor properties. Its π -acceptor capability is only slightly stronger.

In this paper we present a theoretical investigation of a series of BE ligands that are isolobal with CO: BF, BO^- , and BNH_2 . The thermodynamic stability of these complexes will be established beyond doubt. Although it is well-known that bonding to a transition metal fragment can stabilize ligands that are unstable in their free form, as can be seen from SiO, CS, or the more famous example of cyclobutadiene,^[6] the high polarity of these ligands and the build-up of positive charge on

Abstract in Dutch: *De synthese van overgangsmetaal-verbindingen met liganden BE, die via boor gecoördineerd zijn, is in principe haalbaar. Dit blijkt uit ons DFT onderzoek naar de mogelijkheid van de isolobale liganden $\text{AE} = \text{CO}$, BF, BNH_2 , $\text{BN}(\text{CH}_3)_2$ en BO^- om aan een metaal te binden in mono- en binucleaire eerste reeks overgangsmetaal-carbonyl-complexen $[\text{M}(\text{CO})_n(\text{AE})]$, $[\text{Fe}_2(\text{CO})_8(\text{AE})]$ en $[\text{Mn}_2(\text{Cp})_2(\text{CO})_4(\text{AE})]$ ($\text{M} = \text{Cr} - \text{Ni}$). Een gedetailleerde analyse van de $\text{M}(\text{CO})_n - \text{BE}$ binding toont aan dat de BE liganden veel betere σ donoren dan CO en vergelijkbare acceptoren zijn (met uitzondering van BO^- , die door de hoge energie van de π^* LUMO een heel zwakke π acceptor is). De $\text{M}(\text{CO})_n - \text{BE}$ bindingen zijn hierdoor significant sterker dan de vergelijkbare $\text{M}(\text{CO})_n - \text{CO}$ bindingen. De $[\text{Cr}(\text{CO})_5(\text{AE})]$ bindings dissociatie-energieën zijn bijvoorbeeld 41.8 (CO), 62.1 (BF), 72.1 (BNH_2), en $93.4 \text{ kcal mol}^{-1}$ (BO^-). De hoge polariteit van de BE liganden en de opbouw van positieve lading op BE doet een lage kinetische stabiliteit verwachten. Voorstellen om deze voor de BE complexen te verbeteren worden gemaakt. Sterische afscherming van reactieve BE grensorbitalen zou door aanbouw van lijvige liganden aan het metaal fragment kunnen plaatsvinden net als het voor BNR_2 met grote groepen R gebeurt. Maar elektronische stabilisatie van de $[\text{M}] - \text{BE}$ binding lijkt net zo belangrijk te zijn. Wij laten zien, dat binucleaire metaal fragmenten, als $\text{Fe}_2(\text{CO})_8$ en $\text{Mn}_2(\text{Cp})_2(\text{CO})_4$, precies de juiste grensorbitalen hebben om dit te bereiken.*

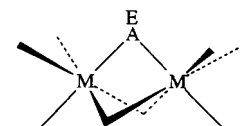
coordination suggest a low kinetic stability for BE complexes. Stable compounds containing boron with the coordination number 2 can be isolated when the boron atom is protected by sterically demanding groups, as can be seen from the iminoboranes $\text{R}-\text{B}=\text{N}-\text{R}'$, where the $\text{B}=\text{N}$ bond is shielded on both sides by large groups R and R'.^[7] However, in transition metal complexes with BO^- or BF ligands protection takes place from only one side and perhaps not very effectively. The analogous organic compounds, the boroxanes $\text{R}-\text{B}=\text{O}$ and borthianes $\text{R}-\text{B}=\text{S}$, are very reactive, and this type of compound is only known in the gas phase, as they trimerize in the condensed phase.^[8,9] A recent investigation succeeded in determining and characterizing the methylboroxide $\text{H}_3\text{C}-\text{B}=\text{O}$,^[10] which is isolobal with the $[(\text{CO})_5\text{Mn}(\text{B}=\text{O})]^{[11]}$ investigated in the present work. The metal organic boroxanes $[\text{L}_n\text{M}(\text{B}=\text{O})]$ could be expected to have reactivities similar to those found for organic boroxanes $\text{R}-\text{B}=\text{O}$.

To overcome the problem of kinetic instability associated with BE complexes, we may invoke both steric protection and better electronic stabilization. The structural features of the BNR_2 ligand (with R potentially bulky) clearly allow for steric protection at the ligand side. Very little is known about BNR_2 , but there is some experimental evidence that indicates that this may be a realistic ligand. In 1970, Schmid, Petz, and Nöth reported^[12] the synthesis of $[\text{Fe}(\text{CO})_4(\text{BNR}_2)]$ ($\text{R} = \text{CH}_3$, C_2H_5). However, these compounds turned out to be thermolabile and oligomerized to give $[\text{Fe}(\text{CO})_4(\text{BNR}_2)]_n$. Braunschweig and Wagner^[13] reported very recently the first X-ray structure of a complex containing the $\text{BN}(\text{CH}_3)_2$ ligand, the binuclear $[\text{Mn}_2(\text{C}_5\text{H}_5)_2(\text{CO})_4\{\text{BN}(\text{CH}_3)_2\}]$. Apart from offering better steric protection at the metal fragment side, there is the interesting possibility of better electronic stabilization provided by binuclear compared with mononuclear metal fragments. The better π -donor capability of fragments such as $\text{Fe}_2(\text{CO})_8$ ^[14] and $\text{Mn}_2(\text{C}_5\text{H}_5)_2(\text{CO})_4$ may play an important role in the electronic stabilization of BE complexes.



Scheme 2. Mononuclear AE complexes.

To answer these and other questions, we have studied the orbital electronic structure of the series of isolobal ligands $\text{AE} = \text{CO}$, BF, BNH_2 , $\text{BN}(\text{CH}_3)_2$, and BO^- , as well as their coordination in mono- (Scheme 2) and binuclear (Scheme 3)



Scheme 3. Binuclear AE complex.

first-row transition metal carbonyl complexes of the type $[\text{M}(\text{CO})_n(\text{AE})]$, $[\text{Fe}_2(\text{CO})_8(\text{AE})]$, and $[\text{Mn}_2(\text{Cp})_2(\text{CO})_4(\text{AE})]$ ($\text{M} = \text{Cr}$, Mn^+ , Fe , Co^+ , Ni), by means of nonlocal density-

functional theory and a large, polarized STO basis set of triple- ζ quality (NL-SCF/TZP).

Experimental Section

General procedure: The calculations reported here were carried out by means of the Amsterdam Density-Functional (ADF) program developed by Baerends et al., vectorized by Ravenek, and parallelized by Fonseca Guerra et al.^[15–18] The MOs were expanded in a large, uncontracted set of Slater-type orbitals (STOs) containing diffuse functions, TZP. The TZP basis set is of triple- ζ quality for all atoms and has been augmented with one set of 4p functions on each transition metal atom, and one set of polarization functions on each main-group atom (2p on H, and 3d on B, C, N, O, and F).^[19,20] The 1s core shell of boron, carbon, nitrogen, oxygen, and fluorine and the 1s2s2p core shells of the first-row transition metal atoms were treated by the frozen-core (FC) approximation.^[15] An auxiliary set of s, p, d, f, and g STOs, centered on all nuclei, was used to fit the molecular density and to represent the Coulomb and exchange potentials accurately in each self-consistent field (SCF) cycle.^[21] The numerical integration was done by means of the scheme developed by te Velde et al.^[18]

All calculations were performed at the NL-SCF level by means of the local density approximation (LDA) in the Vosko–Wilk–Nusair parametrization^[22] with nonlocal corrections for exchange (Becke 88)^[23] and correlation (Perdew 86).^[24] Geometries were optimized by means of the analytical gradient method implemented by Versluis and Ziegler.^[25,26]

Vibrational frequencies^[27] were calculated by numerical differentiation of the analytical energy gradients. For economic reasons, vibrational analyses have only been carried out for the $[\text{Cr}(\text{CO})_5(\text{L})]$ systems ($\text{L} = \text{BF}, \text{BO}^-, \text{BNH}_2, \text{BN}(\text{CH}_3)_2$), which all turn out to be minima on the potential energy surface (PES). Zero-point vibrational energy (ZPE) and thermal energy corrections (for 298.15 K) were previously shown to be on the order of a few kcal mol^{-1} . In the present study they are neglected.

It has been mentioned in a recent investigation that the basis set superposition error (BSSE) could contribute considerably to the calculated bond energy of negatively charged systems by means of DFT methods, and a counter correction of about 20 kcal mol^{-1} was reported for CN^- .^[28] Our studies on the first bond dissociation energy of $[\text{Cr}(\text{CO})_6]^-$ with various basis sets show that the BSSE is smaller than $1.5 \text{ kcal mol}^{-1}$ for the basis set combination used in this investigation.^[29] For $[\text{Cr}(\text{CO})_5(\text{BO})]^-$ a somewhat larger BSSE of 5 kcal mol^{-1} is found with the same basis set combination. However, these values are rather small compared with the overall bond energies, so BSSE corrections are also neglected in this investigation.

Bonding energy analysis: The transition metal boron bond in the various mono- and binuclear complexes was analyzed by means of the well-known breakdown^[30–33] of the interaction energy into an exchange (or Pauli) repulsion and an electrostatic interaction energy term (ΔE^0), and the orbital interaction energy (charge transfer, polarization). It is sometimes necessary to prepare the fragments for interaction, for instance by deforming them from their equilibrium structure to the geometry they acquire in the overall molecule or by electronic excitation to a valence state electronic configuration. The overall bond energy ΔE is thus made up of three major components [Eq. (1)] where $\Delta E^0 = \Delta E_{\text{elst}} + \Delta E_{\text{Pauli}}$.

$$\Delta E = \Delta E_{\text{prep}} + \Delta E^0 + \Delta E_{\text{oi}} \quad (1)$$

Note that ΔE is defined as the negative of the bond dissociation energy BDE, $\Delta E = E(\text{molecule}) - \sum E(\text{fragments}) = -\text{BDE}$, and is negative for a stable bond. ΔE_{elst} (usually attractive) represents the electrostatic interaction between the prepared fragments when they are put, with unchanged electron densities, at the positions they will occupy in the complex. The Pauli repulsion ΔE_{Pauli} comprises the four-electron destabilizing interactions between occupied orbitals and is responsible for the steric repulsion. For neutral fragments, it is useful to combine ΔE_{elst} and ΔE_{Pauli} in the steric interaction term ΔE^0 [Eq. (1)]. The orbital interaction ΔE_{oi} accounts for charge transfer (interaction between occupied orbitals on one moiety with unoccupied orbitals of the other, including the HOMO–LUMO inter-

actions) and polarization (empty/occupied orbital mixing on one fragment). We will not try to separate charge-transfer and polarization components, but we will use the extended transition-state (ETS) method developed by Ziegler and Rauk^[31,32] to split the ΔE_{oi} term into contributions from each irreducible representation Γ of the interacting system [Eq. (2)].

$$\Delta E_{\text{oi}} = \sum_{\Gamma} \Delta E_{\Gamma} \quad (2)$$

In systems with a clear σ, π separation this symmetry partitioning proves to be most informative.

Results and Discussion

Boron ligands BE

Isolobal analogies and differences with CO: In this section, we discuss how our BE model ligands are all isolobal to CO. We will also see how much they can differ, especially when charge effects come into play (as for BO^-).

BF, BNH_2 , and $\text{BN}(\text{CH}_3)_2$: Since the orbital character and energetics of the frontier orbitals, the 5σ HOMO and the 2π LUMOs ($3\sigma_{\text{g}}$ and $1\pi_{\text{g}}$ in N_2), determine the coordination capabilities of the BE molecules, we will discuss these orbitals in some detail, with isolobal N_2 included for comparison. The HOMO of any of these AE diatomics can be viewed as a slightly antibonding A–E lone-pair orbital with an sp_z^x lobe, which participates in the metal-ligand bond through σ donation of charge into an empty d_z hybrid orbital on the metal carbonyl fragment, as shown in Scheme 1, **1**. The antibonding character is reflected in the negative overlap populations, given in Figure 1, which are small and do not change much throughout the series. The two π^* LUMOs, which are much more A–E antibonding than the σ HOMO (note the negative overlap populations), are involved in π back-donation accepting charge from d_{xz} (Scheme 1, **2**) and d_{yz} hybrid orbitals (Scheme 1, **3**). These general features of forward and back-donation are well-known.

How exactly does the AE electronic structure change as we go from N_2 through CO to BF (Figure 1)? The AOs of the electropositive atom A rise in energy and become more diffuse along this series, whereas those of the electronegative atom E decrease in energy and become more compact. This leads to an energy mismatch, poorer overlaps, and therefore to weaker A–E orbital interactions. As a consequence the bonding 1π orbital localizes on the more electronegative E atom whilst the $2\pi^*$ LUMOs, $2p_{\pi}(\text{A}) - 2p_{\pi}(\text{E})$, drop slightly in energy and become more localized on A (Figure 1). The HOMO in N_2 is zero-order $2p_z(\text{A}) + 2p_z(\text{E})$ with an antibonding admixture of $2s(\text{A}) + 2s(\text{E})$. As we go to CO and BF, the HOMO character shifts more and more toward $2s(\text{A}) - 2p_z(\text{E})$ with a bonding admixture of $2p_z(\text{A})$. This ligand donor orbital in fact becomes very localized on A and increases rather strongly in energy (Figure 1). The higher amplitude of both HOMO and LUMO on A will increase the interaction with the metal carbonyl fragment, as indicated by the overlaps with the metal-fragment acceptor orbital quoted in angular brackets in Figure 1. It is clear that the important jump is from N_2 to CO. The lack of amplitude of the frontier orbitals of N_2

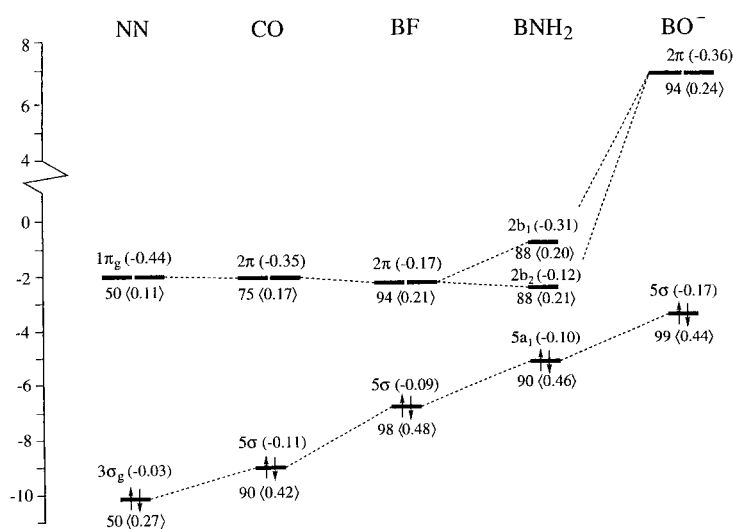
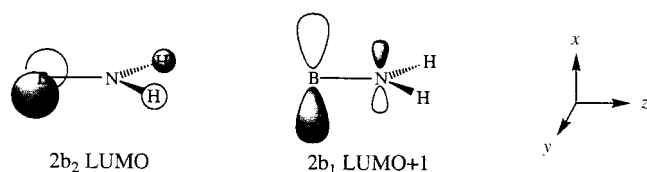


Figure 1. Valence orbital energies (eV) of AE systems N_2 , CO, BF, BNH_2 , and BO^- . Below each level the percentage of atom A character is indicated and the overlaps with the relevant $Fe(CO)_4$ frontier orbital are quoted in angular brackets. Above each level the Mulliken overlap population is given in parentheses.

at the coordinating atom and the concomitant poor overlap with the metal fragment are aggravated by the low energetic position of the σ HOMO. The AE ligand's overall metal-binding ability is thus expected to increase in the order $N_2 \leq CO < BF < BNH_2$, and along this series the importance of σ donation should be enhanced relative to that of π back-donation. These expectations have been checked (preliminary communication see ref. [4]) and will be verified more fully in later sections.

As noted in the introduction, C_{2v} -symmetrical BNH_2 may be an interesting alternative to the reactive BF in view of possibilities for steric protection by bulky substituents. Its frontier-orbital energies suggest that it has even better ligating properties than BF (Figure 1). The $5a_1$ HOMO is higher in energy and the $2b_2$ LUMO, the π^* orbital lying in the molecular plane, is lower in energy. Let us have a closer look at the $2b_1$ and $2b_2$ MOs of BNH_2 . One can view them as being derived from the degenerate π_x^* and π_y^* MOs of the BN fragment, $2p_x(B) - 2p_x(N)$ and $2p_y(B) - 2p_y(N)$, respectively. The latter is stabilized through a bonding interaction with the out-of-phase combination of the two hydrogen 1s AOs and becomes the $2b_2$ LUMO. At the same time, an antibonding second-order admixture of BN π_y , $2p_y(B) + 2p_y(N)$, enhances the amplitude on B and virtually cancels that on N (Scheme 4).



Scheme 4. LUMO orbitals of BNH_2 .

The BN π_x^* or $2p_x(B) - 2p_x(N)$ cannot be stabilized by the hydrogen 1s AOs, because it is orthogonal to them. Therefore, it remains at higher energy (Figure 1) and becomes the $2b_1$ LUMO+1 (Scheme 4). An alternative but equivalent perspective arises if one analyses BNH_2 in terms of B and NH_2 . The $2b_2$ is then the free $2p_y$ AO of boron (almost unperturbed by the NH_2 fragment), whereas the $2b_1$ is the boron $2p_x$ AO, destabilized by the $2p_x(N)$ -like $1b_1$ MO of NH_2 . Besides gauging it against CO, it is interesting to compare BNH_2 with the vinylidene ligand CCH_2 , which is known to form stable transition metal complexes. The HOMO–LUMO gap of 3.0 eV is nearly identical and the CCH_2 $3a_1$ HOMO (83%) and $2b_2$ LUMO (80%) are somewhat less localized on the terminal atom, in line with the reduced electronegativity difference between the two main-group atoms.

The BO^- ligand is clearly the odd one out in the present series. Even though its frontier orbitals 5σ and $2\pi^*$ are similar in shape to those of the other BE ligands, as judged by the degree of localization and the overlaps with the metal-fragment frontier orbitals, the energy of the BO^- orbitals shift considerably, the $2\pi^*$ to quite high energy, owing to the negative charge. The fact that the occupied 1π (not shown in Figure 1) actually reverses its position with respect to the 5σ , becoming the de facto HOMO, is of minor importance since it has a small amplitude at B (18%) and a small overlap (0.04) with the metal-fragment HOMO. The orbital energies in the isolated ligand have to be viewed with some caution, since complexation will reduce the negative charge considerably and therefore lower the effective orbital energies. It is nevertheless evident that BO^- will be a very poor π acceptor; on the other hand it may be expected to be a very good σ donor.

Metal–boron coordination in mononuclear complexes: We have made a comparison between the various ligands, in particular with respect to σ bonding and π back-bonding capabilities, by means of a detailed bond-energy deconstruction. However, these energy components are not observable, and we will first discuss trends for a number of experimentally observable quantities such as geometries, frequencies, and bond enthalpies, which are generally used to make inferences about trends in σ donation and π back-donation.

Geometries, frequencies and bond enthalpies: An often used indicator of the relative π -acceptor strength of a ligand is the geometry change of the carbonyl groups attached to the same metal, notably the one in the *trans* position. The C–O bond is lengthened and its force constant is lowered by back-bonding. These observables may be used to monitor the π -acceptor strength of the AE ligands, since a good AE π acceptor reduces the amount of back-bonding to the other (carbonyl) ligands, leading to a shorter C–O distance and higher frequency. Of course, the A–E bond length itself is the primary geometric parameter to reflect bonding effects. In view of the larger negative overlap population of the $2\pi^*$ orbitals compared with the 5σ HOMO, π back-bonding will have the strongest effect (the overlap populations are given in Figure 1 in parentheses). This will have the effect of lengthening the bond, while σ donation, depopulating the (weakly)

antibonding HOMO, will tend to shorten the bond, in particular in BO^- with its relatively strongly antibonding 5σ .

The calculated geometries of the mononuclear carbonyl compounds $[\text{M}(\text{CO})_n-(\text{AE})]$ ($\text{M} = \text{Cr}, \text{Mn}, \text{Fe}, \text{Co},$ and Ni) are listed together in Table 1. For the complexes derived from $\text{Fe}(\text{CO})_5$ and $\{\text{Co}(\text{CO})_5\}^+$ these geometries represent the trigonal bipyramidal conformations, where the substituent is in the axial position. Substitution at the equatorial position leads to conformations that are 2–5 kcal higher in energy for all of the investigated ligands. In case of $\text{AE} = \text{BNH}_2$ a very low rotation barrier around the $\text{M}-\text{B}-\text{N}$ axis is found that is less than $0.5 \text{ kcal mol}^{-1}$. This is in agreement with theoretical and experimental data for complexes of the isoelectronic vinylidene ligand (CCH_2) .^[34,35] The structural parameters of the eclipsed conformations are given in Table 1; the values of the equatorial carbonyls are averaged for the CO groups parallel and perpendicular to the NH_2 plane. The definitions of the angles α and β are shown in Figure 2.

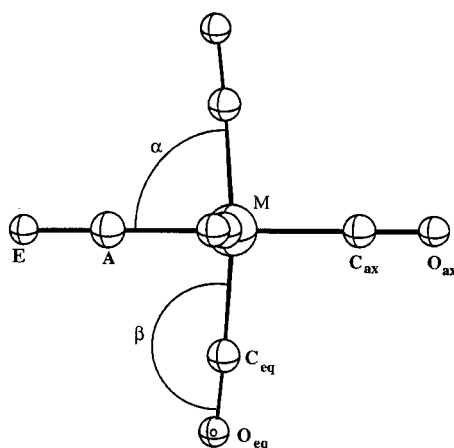


Figure 2. Definition of structural parameters of mononuclear $[\text{M}(\text{CO})_n-(\text{AE})]$ complexes.

Table 1. Selected bond lengths (\AA) and angles ($^\circ$) of $[\text{M}(\text{CO})_n-(\text{AE})]$ ($\text{M} = \text{Cr}, \text{Mn}, \text{Fe}, \text{Co}, \text{Ni}; n = 5, 4, 3$).

		$r(\text{M}-\text{A})$	$r(\text{A}-\text{E})$	$r(\text{M}-\text{C})_{\text{trans}}$	$r(\text{C}-\text{O})_{\text{trans}}$	$r(\text{M}-\text{C})_{\text{cis}}$	$r(\text{C}-\text{O})_{\text{cis}}$	α	β
$\text{Cr}(\text{CO})_5$	–CO	1.927	1.155	1.927	1.155	1.927	1.155	90.0	180.0
$\{\text{Mn}(\text{CO})_5\}^+$	–CO	1.894	1.141	1.894	1.141	1.894	1.141	90.0	180.0
$\text{Fe}(\text{CO})_4$	–CO	1.821	1.153	1.821	1.153	1.820	1.156	90.0	180.0
$\{\text{Co}(\text{CO})_4\}^+$	–CO	1.834	1.139	1.834	1.139	1.877	1.139	90.0	180.0
$\text{Ni}(\text{CO})_3$	–CO	1.841	1.151	1.841	1.151	1.841	1.151	109.5	180.0
free ligand	CO		1.138						
$\text{Cr}(\text{CO})_5$	–BF	1.909	1.281	1.923	1.153	1.914	1.157	87.8	178.1
$\{\text{Mn}(\text{CO})_5\}^+$	–BF	1.886	1.259	1.913	1.139	1.894	1.147	88.0	178.0
$\text{Fe}(\text{CO})_4$	–BF	1.815	1.275	1.838	1.160	1.807	1.160	86.2	178.9
$\{\text{Co}(\text{CO})_4\}^+$	–BF	1.820	1.251	1.863	1.137	1.850	1.142	85.8	179.7
$\text{Ni}(\text{CO})_3$	–BF	1.850	1.274			1.850	1.153	106.7	178.1
free ligand	BF		1.272						
$\text{Cr}(\text{CO})_5$	– BNH_2	1.939	1.379	1.937	1.155	1.912	1.160	87.3	178.2
$\{\text{Mn}(\text{CO})_5\}^+$	– BNH_2	1.924	1.354	1.937	1.142	1.885	1.145	87.7	178.3
$\text{Fe}(\text{CO})_4$	– BNH_2	1.848	1.378	1.840	1.157	1.804	1.164	86.3	178.9
$\{\text{Co}(\text{CO})_4\}^+$	– BNH_2	1.858	1.346	1.863	1.138	1.825	1.142	86.4	179.2
$\text{Ni}(\text{CO})_3$	– BNH_2	1.883	1.384			1.852	1.155	108.1	176.4
free ligand	BNH_2		1.380						
$\text{Cr}(\text{CO})_5$	– BO^-	2.098	1.234	1.865	1.173	1.900	1.167	87.6	177.6
$\{\text{Mn}(\text{CO})_5\}^+$	– BO^-	2.051	1.221	1.841	1.151	1.868	1.150	87.3	177.9
$\text{Fe}(\text{CO})_4$	– BO^-	1.973	1.234	1.801	1.169	1.791	1.172	83.9	179.3
$\{\text{Co}(\text{CO})_4\}^+$	– BO^-	1.948	1.220	1.826	1.148	1.816	1.151	83.5	179.0
$\text{Ni}(\text{CO})_3$	– BO^-	2.011	1.235			1.813	1.169	104.1	179.0
free ligand	BO^-		1.247						

Much theoretical work has already been done on structure and bonding of the binary carbonyl compounds of the first-row transition metals.^[36–41] Since we are interested in the changes in the structures caused by substitution, we have repeated these calculations to produce a comparable set of data. Comparisons with experimental data for the mononuclear systems can be found in the above references. They show an excellent agreement for the methods used. We will make a comparison with the experimentally derived values of the binuclear complexes in a later section.

Apart from a comparison amongst the AE ligands, we can also compare the neutral metal carbonyl fragments to the charged ones, the latter presumably amplifying the effect of σ donation and diminishing the π back-donation.

Considering first the complexation with neutral metal carbonyl fragments, we note for CO an increase in bond length ($>0.01 \text{ \AA}$) with respect to the free ligand, for BF a smaller increase in bond length, virtually no change for BNH_2 , and a distinctly shorter bond for BO^- . The smaller increase in bond length for BF than for CO does not necessarily imply weaker back-bonding, since the antibonding character of the $\text{BF } 2\pi^*$ is only half that of CO (cf. Figure 1). We can conclude from these geometry effects that π back-bonding is important for CO and BF, but owing to the opposite effects of σ and π bonds on the geometry and the larger effect of π back-bonding than σ donation, very little can be concluded concerning the relative magnitude of these two types of bond. The absence of any clear geometry effect for the aminoborane complexes, combined with the expectation of similar π back-bonding as for CO and BF based on the similar orbital energies and frontier orbital overlaps, leads us to infer stronger σ donation in this case, which is necessary in order to cancel the bond-lengthening effect of the π back-bonding. This would fit in with the higher HOMO orbital energy. The shorter bond for BO^- is particularly striking. This fits in with

the expected small π back-bonding and strong σ donation on account of the high orbital energies for both these levels.

Upon coordination to the isoelectronic positive metal carbonyl fragments the AE bond lengths become distinctly shorter than when coordinated to the neutral fragments. This is consistent with the expectation of less π back-bonding and stronger σ donation. Both effects tend to strengthen and shorten the AE bond, as is observed in all cases. In fact, for the positive metal fragments there is a net bond shortening with respect to the free ligand for all boron-containing ligands, increasingly so in the series $\text{BF} < \text{BNH}_2 < \text{BO}^-$, but not for CO. This is clear evidence for the increasing importance of σ donation of the BE ligands.

If we compare the other calculated structural parameters of the substituted complexes with those of the binary carbonyl complexes it can be seen from Table 1 that the geometries are hardly affected by the substitution. The angles between the substituents and the equatorial CO, which are still linearly bound, are in all the investigated cases somewhat smaller than in the binary carbonyl compounds. The π back-bonding of the BE ligands apparently differs too little from that of CO to make a significant change to the $\text{C}-\text{O}_{\text{trans}}$ or $\text{C}-\text{O}_{\text{cis}}$ distances, except for BO^- . Here the expectation of poorer π -accepting ability and therefore increased π back-bonding to the other ligands is confirmed by relatively long C–O bond lengths. The structures of the complexes of BO^- are very similar to those of CN^- reported earlier.^[35]

For an additional comparison, we can consider the A–E stretching frequencies. Since frequency calculations with numerical derivatives of the analytical gradients require severe computational effort we will limit our consideration to the comparison of the vibrational frequencies of the free ligands with those of the mononuclear chromium complexes. These stretching frequencies $\tilde{\nu}(\text{A}-\text{E})$ and the calculated frequency shifts are shown in Table 2. No imaginary frequencies are found and all the calculated $[\text{Cr}(\text{CO})_5-(\text{AE})]$ compounds are minima on the potential energy surface.

For $[\text{Cr}(\text{CO})_5(\text{BF})]$ the calculated change of the stretching frequency is in agreement with the results of our previous investigation^[5] of $[\text{Fe}(\text{CO})_4(\text{BF})]$ with $\Delta\tilde{\nu} = 90 \text{ cm}^{-1}$. For $[\text{Cr}(\text{CO})_6]$ the experimental observations are reproduced

Table 2. Calculated vibrational frequencies (cm^{-1}) of the free ligands and of the $[\text{Cr}(\text{CO})_5-(\text{AE})]$ complexes.

	CO	BF	BNH ₂	BO ⁻
$\tilde{\nu}(\text{A}-\text{E})$, free ligand	2124	1358	1238	1686
$\tilde{\nu}(\text{A}-\text{E})$, $[\text{Cr}(\text{CO})_5-(\text{AE})]$	1971	1461	1347	1773
$\Delta\tilde{\nu}$	-153	103	109	87

and a frequency shift of about -150 cm^{-1} is calculated. For the complexes of the other three ligands BF, BNH_2 , and BO^- , the opposite trend is predicted than for CO and the frequencies are shifted by about 100 cm^{-1} towards higher wavenumbers. The relative effects of π back-donation and σ donation are clearly different for the frequencies than for the bond lengths. The frequency shifts show that σ donation exists for all three ligands BO^- , BF, and BNH_2 , and is relatively more important for the BE ligands than for CO. The present results strengthen our interpretation of the structural evidence (decreasing A–E bond lengthening in the series CO, BF, BNH_2) in terms of increasing σ donation rather than decreasing π back-donation. The upward frequency shift for BO^- is in line with the expected strong σ donation, but the fact that it is smaller than in the other BE ligands is hard to reconcile with the particularly large σ donation and very small π back-donation expected for this ligand.

The bond enthalpies ΔH are given in Table 3 (the decomposition of ΔH into various components will be discussed in the next section). In the case of the $\text{Fe}(\text{CO})_4$ fragment we found a $^3\text{b}_2$ triplet ground-state in an earlier investigation with a singlet–triplet excitation energy smaller than 1 kcal mol^{-1} . Since the thermal dissociation with respect to the triplet ground-state is a spin-forbidden process,^[40] the dissociation energies of $[\text{Fe}(\text{CO})_5]$ and the analogue $[\text{Fe}(\text{CO})_4-(\text{AE})]$ refer to the singlet ground-state.

Values for the bond dissociation energies of the binary carbonyl compounds $[\text{Cr}(\text{CO})_6]$, $[\text{Fe}(\text{CO})_5]$, and $[\text{Ni}(\text{CO})_4]$ have been reported earlier both with DFT methods^[40,41] and at the CCSD(T) level of theory,^[38,39] and the reliability of the present DFT method has been established in extensive validation against experimental data. The value of the bond dissociation of $[\text{Fe}(\text{CO})_5]$ ($\Delta H = 48.4 \text{ kcal mol}^{-1}$) is somewhat

Table 3. Calculated bond dissociation enthalpies and energy decomposition (kcal mol^{-1}).

	$[\text{Cr}(\text{CO})_5(\text{AE})]$	$[\text{Mn}(\text{CO})_5]^+\text{AE}$	$[\text{Fe}(\text{CO})_4(\text{AE})]$	$[\text{Co}(\text{CO})_4]^+\text{AE}$	$[\text{Ni}(\text{CO})_3(\text{AE})]$	$[\text{Fe}_2(\text{CO})_8(\text{AE})]$	$[\text{Mn}_2(\text{Cp})_2(\text{CO})_4(\text{AE})]$	
CO	-BDE (ΔH)	-41.8	-44.2	-48.4	-37.3	-28.2	-30.6	-48.3
	$\Delta E^0 + \Delta E_{\text{prep}}$	30.5	28.7	38.1	43.8	32.9	73.9	84.1
	ΔE_{σ}	-33.8	-43.2	-44.8	-51.8	-28.0	-49.3	-45.0
	ΔE_{π}	-38.5	-29.7	-41.7	-29.3	-33.1	-55.2	-87.4
BF	-BDE (ΔH)	-62.1	-71.4	-73.8	-70.6	-45.3	-71.0	-90.2
	$\Delta E^0 + \Delta E_{\text{prep}}$	38.9	36.8	54.2	63.4	20.0	85.8	99.8
	ΔE_{σ}	-59.0	-75.8	-81.7	-100.1	-38.8	-87.5	-97.2
	ΔE_{π}	-42.0	-32.4	-46.3	-33.9	-34.5	-69.3	-92.8
BNH ₂	-BDE (ΔH)	-72.1	-94.4	-87.7	-98.6	-52.7	-72.8	-97.3 (-92.3)
	$\Delta E^0 + \Delta E_{\text{prep}}$	31.6	20.0	42.2	41.4	17.6	68.2	98.7 (84.9)
	ΔE_{σ}	-67.1	-86.2	-89.6	-110.0	-40.9	-88.3	-108.0 (-97.7)
	ΔE_{π}	-36.6	-28.2	-40.3	-30.0	-29.4	-52.7	-88.0 (-79.5)
BO ⁻	-BDE (ΔH)	-93.4	-206.1	-106.1	-216.6	-70.0	-102.0	-90.7
	$\Delta E^0 + \Delta E_{\text{prep}}$	-3.2	-88.9	26.2	-54.0	-0.8	37.1	49.1
	ΔE_{σ}	-75.6	-101.9	-112.2	-141.5	-61.1	-113.9	-102.0
	ΔE_{π}	-14.6	-16.1	-20.1	-21.1	-8.1	-25.2	-37.8

larger than the value reported in our previous study^[5] on substituted iron carbonyl complexes ($\Delta H = 44.6 \text{ kcal mol}^{-1}$) with a different basis set. It is well-known that among the neutral compounds $[\text{Ni}(\text{CO})_4]$ has the weakest metal–carbonyl bond strength ($28.2 \text{ kcal mol}^{-1}$), the bond to the $\text{Cr}(\text{CO})_5$ fragment being quite a bit stronger ($41.8 \text{ kcal mol}^{-1}$), and to $\text{Fe}(\text{CO})_4$ clearly the strongest ($48.4 \text{ kcal mol}^{-1}$).

The calculated bond energies (Table 3) show that the transition metal boron bond in all cases is thermodynamically more stable than the corresponding metal–carbonyl bond. For each BE ligand the trend with the metal carbonyl fragments is the same as for CO but with more pronounced differences. Among the BE ligands the bond strength increases from BF to BNH_2 to BO^- . The M–BF bond is predicted to be 1.5–2 times stronger than the corresponding carbonyl bond. For complexes of BNH_2 ΔH is greater by 10–28 kcal mol^{-1} with respect to BF. The bonds to BO^- are the strongest. For the neutral metal carbonyl fragments the increase with respect to BNH_2 is again approximately 20 kcal mol^{-1} , but for the positive metal carbonyl fragments the electrostatic effects lead to a jump of more than 100 kcal mol^{-1} .

The increase in bond enthalpy is consistent with the increasing contribution of σ bonding that we inferred above, although it is surprising that the expected reduced π bonding for BO^- seems to have so little effect on the total bond strength for this ligand. We conclude that the experimentally observable quantities that we have investigated in this section give consistent but not conclusive evidence for the expected trends in the bonding mechanisms.

Electronic structure and bonding: Table 3 also contains the breakdown of the total bond enthalpies into the term ΔE_σ representing the σ donation, the term ΔE_π representing the π back-bonding and the term $\Delta E^0 + \Delta E_{\text{prep}}$. ΔE^0 summarizes the attractive electrostatic interaction ΔE_{elst} and the repulsive Pauli repulsion ΔE_{Pauli} . ΔE_{prep} is the energy difference between the ground states of the fragments at their equilibrium structure and the valence states of the fragments at the geometries they possess in the complex (the preparation energy). These energy components provide quantitative underpinning for the inferences we have made concerning the contributions to the bond energy. The assumption that the π bonding is comparable in CO, BF, and BNH_2 is corroborated by the fact that for each of the mononuclear metal carbonyl fragments the ΔE_π terms for these ligands are similar (for $\text{Cr}(\text{CO})_5$: -38.5 , -42.0 , and $-36.6 \text{ kcal mol}^{-1}$, respectively). As expected ΔE_π for BO^- ($-14.6 \text{ kcal mol}^{-1}$ for $\text{Cr}(\text{CO})_5$) is much smaller. The σ bonding, on the other hand, exhibits a clear increase in the series, the largest increase occurring on going from CO to BF (25 kcal mol^{-1} for $\text{Cr}(\text{CO})_5$), with subsequent steps of ca. 8 kcal mol^{-1} to BNH_2 and then to BO^- . The $\Delta E^0 + \Delta E_{\text{prep}}$ term is positive (repulsive) owing to the Pauli repulsion, which does not vary much throughout the BE series. The attractive electrostatic term, however, is much more stabilizing in the case of the charged BO^- fragment, hence the reduction of this term (to almost zero for the $\text{Cr}(\text{CO})_5$ and $\text{Ni}(\text{CO})_3$ fragments). The picture is now rather simple: the increasing bond enthalpy in the series

is caused primarily by increasing σ bonding. In the case of BO^- the sharp decrease of the π bonding is overcompensated, mostly by much greater electrostatic attraction in addition to an increase in σ bonding.

In going from the neutral to the corresponding positive metal carbonyl fragments we find the expected larger σ bonding (the increase ranging between 10 and 30 kcal mol^{-1}) and the expected decrease in π bonding, although the latter is more modest (the decrease is always in the order of 10 kcal mol^{-1} , and only a few kcal mol^{-1} for BO^-). The very strong bond of BO^- to these positive fragments, which seems to be somewhat unusual, is simply caused by electrostatic effects between the charged fragments.

The data in Table 3 also introduce the possibility to order the transition metal carbonyl fragments according to their bonding capabilities. $\text{Ni}(\text{CO})_3$, with a formally occupied 3d shell, is not only the weakest σ acceptor, but also has weak π -back-bonding capability compared with the other neutral metal carbonyl fragments. Since the orbital energies and the overlap integrals of the π -donor orbitals in $\text{Ni}(\text{CO})_3$, $\text{Fe}(\text{CO})_4$ and $\text{Cr}(\text{CO})_5$ fragments are comparable, the small π back-donation of the $[\text{Ni}(\text{CO})_3-(\text{AE})]$ complexes is possibly a result of (lack of) synergism with σ donation. In $[\text{Cr}(\text{CO})_6]$, synergism of σ and π bonding has been shown to increase electronic interaction energies by ca. 50%.^[36] The $\text{Fe}(\text{CO})_4$ fragment is a particularly good σ acceptor (for the BE ligands about twice as effective as $\text{Ni}(\text{CO})_3$) and usually also the best π donor, but only with a small margin of a few kcal mol^{-1} . The positive metal carbonyl fragments behave as expected: by far the best σ acceptor is $\{\text{Co}(\text{CO})_4\}^+$.

This theoretical investigation gives a bright picture of the experimental accessibility of organometallic complexes containing BF, BNR_2 , and BO^- as alternative ligands to the isoelectronic carbon monoxide. High bonding energies are computed and the complexes are predicted to be thermodynamically more stable than those of CO. However, this does not necessarily mean that those complexes will be kinetically stable. The boron atom is susceptible to nucleophilic attack owing to the high amplitude of the 2π orbital of B (orbital control), to which is added the effect of a considerably more positive charge on B (charge control). The calculated Hirshfeld charges^[42] on the A atom are presented in Table 4. As expected, our calculations demonstrate this charge effect to be small or even in the opposite (negative) direction in the case of the CO ligand, but considerable and increasing in the series $\text{BF} < \text{BNH}_2 < \text{BO}^-$. In the next section we address the question of how to achieve complexation of BE ligands with improved kinetic stability.

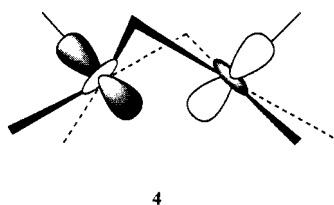
Table 4. Calculated Hirshfeld charges^[42] on A.

	CO	BF	BO	BNH_2
AE	+0.08	+0.07	-0.50	+0.06
$[\text{Cr}(\text{CO})_5-(\text{AE})]$	+0.06	+0.15	+0.02	+0.09
$[\text{Mn}(\text{CO})_5]^+-(\text{AE})$	+0.17	+0.28	+0.11	+0.21
$[\text{Fe}(\text{CO})_4-(\text{AE})]$	+0.10	+0.20	+0.09	+0.17
$[\{\text{Co}(\text{CO})_4\}^+-(\text{AE})]$	+0.19	+0.32	+0.13	+0.26
$[\text{Ni}(\text{CO})_3-(\text{AE})]$	+0.05	+0.10	+0.01	+0.06
$[\text{Fe}_2(\text{CO})_8-(\text{AE})]$	+0.09	+0.15	+0.08	+0.15
$[\text{Mn}_2(\text{Cp})_2(\text{CO})_4-(\text{AE})]$	+0.05	+0.09	+0.06	+0.05

Metal–boron coordination in binuclear complexes

The binuclear $\text{Fe}_2(\text{CO})_8$ and $\text{Mn}_2(\text{Cp})_2(\text{CO})_4$ fragments: There are several possible strategies to enhance the kinetic stability of BE complexes. Steric shielding of the B atom can be accomplished by coordination to a sterically better protected metal fragment. In the case of BNH_2 there is the possibility to enhance steric protection by substituting the H's with bulky groups. Electronic factors may also be brought into play. If the metal fragment is an exceptionally strong π donor, the coordinative bond will be strengthened but also the ligand 2π orbital will be shifted strongly upwards by antibonding with the occupied π -donor orbital. The very high energy of this acceptor orbital of the complex will be an impediment to nucleophilic attack at the B atom. Strong π back-donation is also beneficial from the point of view of charge control, since it will counteract the positive charge effect of the strong σ donation.

Coordination of the BE ligands at a bridging position in a binuclear complex, to form for instance $[\text{Fe}_2(\text{CO})_8-(\text{BE})]$ and $[\text{Mn}_2(\text{Cp})_2(\text{CO})_4-(\text{BE})]$ (Cp = cyclopentadienyl), would be a way to achieve the desired goals. Steric protection is evidently better than in a mononuclear complex. Moreover it is known that the π -bonding capability of these metal fragments is exceptionally good. This has been evident for a long time from the low CO vibration frequency for a bridging CO. The frontier orbitals of the $\text{Fe}_2(\text{CO})_8$ fragment—in the conformation found in $[\text{Fe}_2(\text{CO})_9]$ —and its σ bonding and π -back-bonding capabilities have been studied in detail.^[14] The exceptionally good π -donating capability of the $\text{Fe}_2(\text{CO})_8$ fragment can easily be rationalized by the fact that the π back-bonding to the bridging ligand will occur out of an orbital that can be characterized as an antibonding combination of two d_{z^2} -like hybrids on the two irons, which are pointing towards the bridging ligand (Scheme 5, 4).



Scheme 5. π back-bonding to the bridging ligand in a binuclear iron complex.

Each Fe atom is octahedrally surrounded by ligands. The π -donor orbital 4 (called the antibonding bent bond orbital BB^* in ref. [14]) is effective since it is a high-lying e_g -type metal d orbital in the local octahedron (usually π -donor d orbitals are low-lying t_{2g} -like stabilized for instance by π back-bonding to surrounding CO ligands as in $\text{Cr}(\text{CO})_5$). The antibonding between the two d_{z^2} -like hybrids helps to raise the energy. As a matter of fact, the bonding equivalent of 4, the bonding bent bond orbital BB, is at lower energy and is occupied in the ground configuration of the $\text{Fe}_2(\text{CO})_8$ fragment. Excitation from the $(\text{BB})^2(\text{BB}^*)^0$ configuration to the $(\text{BB})^0(\text{BB}^*)^2$ valence state configuration has to take place in the $\text{Fe}_2(\text{CO})_8$ fragment

to prepare it for bonding with a σ -donating, π -accepting ligand. The corresponding electronic excitation energies of about 29 kcal mol^{-1} for $\text{Fe}_2(\text{CO})_8$ and 17 kcal mol^{-1} for $\text{Mn}_2(\text{Cp})_2(\text{CO})_4$ have been added to the preparation energy ΔE_{prep} and contribute to the rather large total $\Delta E^0 + \Delta E_{\text{prep}}$ term for the binuclear metal fragments (see Table 3 and discussion below). We refer to ref. [14] for contour plots of the relevant orbitals and an extensive discussion of the electronic structure of the $\text{Fe}_2(\text{CO})_8$ fragment and its bonding behaviour in compounds such as $[\text{Fe}_2(\text{CO})_8-(\text{CO})]$, $[\text{Fe}_2(\text{CO})_8(\text{CCH}_2)]$ and $[\text{Fe}_2(\text{CO})_8-\text{Fe}(\text{CO})_4]$.

Since the binuclear fragments $\text{Fe}_2(\text{CO})_8$ and $\text{Mn}_2(\text{Cp})_2(\text{CO})_4$ are very interesting for steric and electronic reasons, and to make a connection with the experimental results for the only known BE complex $[\text{Mn}_2(\text{Cp})_2(\text{CO})_4\{\text{BN}(\text{CH}_3)_2\}]$, we consider in this section the complexes $[\text{Fe}_2(\text{CO})_8-(\text{BE})]$ and $[\text{Mn}_2(\text{Cp})_2(\text{CO})_4-(\text{BE})]$. Both fragments $\text{Mn}_2(\text{Cp})_2(\text{CO})_4$ and $\text{Fe}_2(\text{CO})_8$ are isolobal in the sense of Hoffmann,^[11] and the electronic structure of $\text{Mn}_2(\text{Cp})_2(\text{CO})_4$ is characterized by very similar types of frontier orbitals. The one-electron energy of the $\text{Fe}_2(\text{CO})_8$ BB^* orbital is some 0.7 eV above the d_{π} orbitals of the mononuclear fragments. The analogous orbital of $\text{Mn}_2(\text{Cp})_2(\text{CO})_4$ is 1.8 eV higher in energy. The overlapping of the $2\pi^*$ BE orbitals with the π -donor orbitals of the binuclear fragments is 10–20% larger than with those of the mononuclear fragments. Thus the $\text{Fe}_2(\text{CO})_8$ and in particular $\text{Mn}_2(\text{Cp})_2(\text{CO})_4$ fragments may be expected to be the better π donors.

Geometries: The structures of the binuclear carbonyl compounds $[\text{Fe}_2(\text{CO})_8-(\text{AE})]$ and $[\text{Mn}_2(\text{Cp})_2(\text{CO})_4-(\text{AE})]$, with AE in the bridging position between the two transition metal centres, are depicted in Figures 3 and 4.

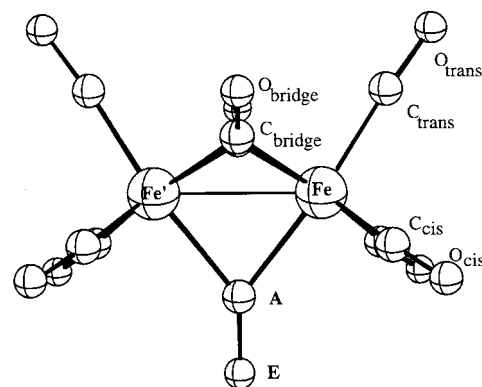


Figure 3. Definition of structural parameters of binuclear complexes $[\text{Fe}_2(\text{CO})_8(\text{AE})]$.

The structural parameters of diiron-nonacarbonyl and the substituted analogues are presented in Table 5. The X-ray diffraction data indicate C_{3h} molecular symmetry with only a small deviation from D_{3h} symmetry, and we applied the latter for the geometry optimisations. Comparison of the theoretical and experimental structural parameters (Table 5, experimental values in parentheses)^[43] show very good agreement for $[\text{Fe}_2(\text{CO})_9]$. The calculated iron–iron distance of 2.545 Å is

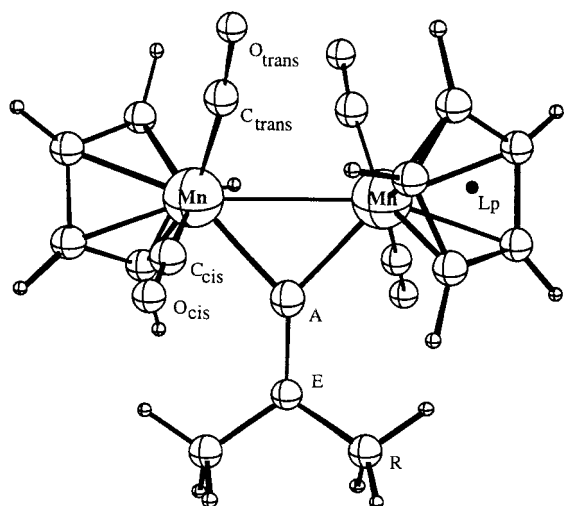


Figure 4. Definition of structural parameters of binuclear complexes $[\text{Mn}_2(\text{Cp})_2(\text{CO})_4(\text{AE})]$.

slightly longer (0.02 Å) than the experimental one. The predicted distances between iron and the bridging carbonyls, 2.028 Å, are also a little bit longer than the experimental value of 2.013 Å, while the experimental distances between iron and the terminal carbonyls are perfectly reproduced by the calculation. The longer C–O distances for the bridging carbonyls compared to the terminal carbonyls, indicating stronger π back-donation at this position, are also reproduced very well, and the difference between theoretically and experimentally derived C–O distances is smaller than 0.004 Å. This is remarkable since the CO-distances of mononuclear transition metal carbonyl complexes are often somewhat overestimated. The deviation of the calculated bond angles is less than 1°, with the exception of the Fe–C–O angle of the terminal carbonyls with a maximum deviation of 2°.

Substitution of one bridging CO by one of the BE ligands leads to a C_{2v} molecular symmetry for $[\text{Fe}_2(\text{CO})_8(\text{BE})]$. In the case of $\text{BE} = \text{BF}$ the iron–iron and the iron–CO_{bridge} distances stay almost the same as in $[\text{Fe}_2(\text{CO})_9]$. The bond to the terminal CO in the *trans* position is slightly longer and that of the *cis*-carbonyl marginally smaller after substitution. The CO distances are almost identical with those in $[\text{Fe}_2(\text{CO})_9]$ and the bond angles are only very slightly affected by substitution. The B–F distance is longer than in the free ligand and in fact slightly longer than in any of the mononuclear complexes.

The same observations can be made when a bridging CO is substituted by BNH_2 . The B–N distance is longer than in any mononuclear complex and the structural parameters of the $\text{Fe}_2(\text{CO})_8$ fragment are the same as in $[\text{Fe}_2(\text{CO})_9]$.

Larger changes are predicted when the substituent is BO^- . The Fe–Fe bond is the longest of the investigated series. The Fe–BO bond is approximately 0.16 Å longer than the corresponding Fe–CO bond and is also the longest in the series. The $\text{Fe}_2(\text{CO})_8$ fragment is also now affected; the metal–CO bond lengths of the terminal CO in the *trans* position, of those in the *cis* position, and of the bridging carbonyls are shorter than in $[\text{Fe}_2(\text{CO})_9]$, whereas the C–O bond lengths are clearly longer. All these observations fit in with comparable π back-bonding with CO and the ligands BF and BNH_2 , and much smaller back-bonding than with BO^- .

The optimized geometries of the $[\text{Mn}_2(\text{Cp})_2(\text{CO})_4(\text{AE})]$ compounds are given in Table 6. We added the dimethyl aminoborane group BNMe_2 to the series of the investigated ligands complexed to the dimanganese cluster. Braunschweig and Wagner synthesized the first stable borylene complexes of the type $[\mu\text{-BX}\{(\eta^5\text{-C}_5\text{H}_4\text{R})\text{Mn}(\text{CO})_2\}_2]$ with $\text{X} = \text{NMe}_2$ and $\text{R} = \text{H}, \text{Me}, t\text{Bu}$, and were able to characterize the structure of $[\mu\text{-BNMe}_2\{(\eta^5\text{-C}_5\text{H}_5)\text{Mn}(\text{CO})_2\}_2]$ by X-ray crystallography.^[13] This is the only set of experimentally derived structural

Table 5. Bond lengths (Å) and angles (°) of $[\text{Fe}_2(\text{CO})_8(\text{AE})]$.^[a]

	$[\text{Fe}_2(\text{CO})_8(\text{CO})]$	$[\text{Fe}_2(\text{CO})_8(\text{BF})]$	$[\text{Fe}_2(\text{CO})_8(\text{BNH}_2)]$	$[\text{Fe}_2(\text{CO})_8(\text{BO})^-]$
$r(\text{M}-\text{M}')$	2.545 (2.523)	2.541	2.545	2.557
$r(\text{M}-\text{C}_{\text{bridge}})$	2.028 (2.013)	2.026	2.017	2.005
$r(\text{M}-\text{AE})$	2.028 (2.013)	2.000	2.065	2.183
$r(\text{M}-\text{C}_{\text{trans}})$	1.838 (1.838)	1.847	1.843	1.802
$r(\text{M}-\text{C}_{\text{cis}})$	1.838 (1.838)	1.823	1.824	1.816
$r(\text{C}_{\text{bridge}}-\text{O})$	1.172 (1.176)	1.173	1.175	1.184
$r(\text{A}-\text{E})$	1.172 (1.176)	1.297	1.400	1.240
$r(\text{C}_{\text{trans}}-\text{O}_{\text{trans}})$	1.153 (1.156)	1.153	1.154	1.165
$r(\text{C}_{\text{cis}}-\text{O}_{\text{cis}})$	1.153 (1.156)	1.155	1.157	1.162
$\alpha(\text{M}-\text{C}_{\text{bridge}}-\text{M}')$	77.7 (77.6)	77.7	78.3	79.2
$\alpha(\text{M}-\text{A}-\text{M}')$	77.7 (77.6)	78.9	76.1	71.7
$\alpha(\text{M}-\text{C}_{\text{bridge}}-\text{O})$	141.1 (141.2)	141.1	140.8	140.4
$\alpha(\text{M}-\text{A}-\text{E})$	141.1 (141.2)	140.6	141.9	144.2
$\alpha(\text{M}-\text{M}'-\text{C}_{\text{trans}})$	121.8 (120.9)	120.9	120.3	121.0
$\alpha(\text{M}-\text{M}'-\text{C}_{\text{cis}})$	121.8 (120.9)	119.3	120.8	116.8
$\alpha(\text{M}-\text{C}_{\text{trans}}-\text{O}_{\text{trans}})$	175.2 (177.1)	178.2	176.9	178.2
$\alpha(\text{M}-\text{C}_{\text{cis}}-\text{O}_{\text{cis}})$	175.2 (177.1)	177.7	176.5	177.1
$\tau(\text{A}-\text{M}-\text{M}'-\text{C}_{\text{bridge}})$	120.0	119.2	118.6	119.9
$\tau(\text{A}-\text{M}-\text{M}'-\text{C}_{\text{trans}})$	180.0 (179.3)	180.0	180.0	180.0
$\tau(\text{A}-\text{M}-\text{M}'-\text{C}_{\text{cis}})$	60.0	57.6	58.7	56.7

[a] Experimental values in parentheses are taken from ref. [42].

Table 6. Optimized bond lengths (Å) and angles (°) of $[\text{Mn}_2(\text{Cp})_2(\text{CO})_4-(\text{AE})]$.^[a]

	AE = CO	AE = BO ⁻	AE = BF	AE = BNH ₂	AE = BNMe ₂
$r(\text{Mn}-\text{Mn})$	2.808	2.853	2.841	2.826	2.827 (2.790)
$r(\text{Mn}-\text{A})$	1.989	2.151	1.977	2.017	2.049 (2.03)
$r(\text{Mn}-\text{C}_{\text{tr}})$	1.792	1.769	1.799	1.791	1.791 (1.78)
$r(\text{Mn}-\text{C}_{\text{cis}})$	1.777	1.758	1.764	1.761	1.760 (1.74)
$r(\text{Mn}-\text{Lp})$	1.811	1.814	1.795	1.802	1.801 (1.783)
$r(\text{C}-\text{O}_{\text{tr}})$	1.171	1.184	1.170	1.172	1.172 (1.17)
$r(\text{C}-\text{O}_{\text{cis}})$	1.170	1.182	1.175	1.177	1.178 (1.17)
$r(\text{A}-\text{E})$	1.192	1.256	1.329	1.405	1.411 (1.39)
$\alpha(\text{Mn}-\text{Mn}-\text{A})$	45.1	48.5	44.1	45.5	46.4 (46.6)
$\alpha(\text{Mn}-\text{A}-\text{Mn})$	89.8	83.0	91.8	89.0	87.2 (86.8)
$\alpha(\text{Mn}-\text{C}-\text{O}_{\text{tr}})$	172.9	172.9	174.5	174.0	173.2 (174.5)
$\alpha(\text{Mn}-\text{C}-\text{O}_{\text{cis}})$	179.2	178.3	178.4	178.9	178.7 (177.9)
$\tau(\text{E}-\text{A}-\text{Mn}-\text{C}_{\text{tr}})$	143.5	140.7	142.2	141.3	141.4 (141.4)
$\tau(\text{E}-\text{A}-\text{Mn}-\text{C}_{\text{cis}})$	60.2	61.3	59.1	59.4	61.5 (62.1)
$\tau(\text{E}-\text{A}-\text{Mn}-\text{Lp})$	297.8	298.7	298.9	298.9	298.9 (298.5)
$\tau(\text{Mn}-\text{A}-\text{E}'-\text{R})$	-	-	-	13.6	7.7 (8.0)

[a] Experimental values in parentheses from ref. [13].

parameters (Table 6, values in parentheses) of the boron-containing carbonyl derivatives with which we can compare our calculated results.

As can be seen from Table 6, the experimentally derived and the theoretically predicted structural parameters are in very good agreement. The calculated Mn–Mn bond distance (2.827 Å) is a little longer than the experimental one (2.790 Å), the deviation of the other bond distances is less than 0.02 Å, and the deviation of the bond angles is about 1°. The relative orientation of the carbonyl groups and the cyclopentadienyl (Cp) ring to the BNMe₂ group are in excellent agreement with the experimental structures as well as the torsion angle $\tau(\text{Mn}-\text{A}-\text{E}-\text{R})$ between the Mn–B–Mn plane and the plane of the trigonal planar coordinated nitrogen. If one compares the calculated structures of complexes of the BNR₂ group, a shorter Mn–B distance ($r(\text{Mn}-\text{B}) = 2.017$ Å) is found for the case R = H than for R = Me ($r(\text{Mn}-\text{B}) = 2.049$ Å) and the torsion angle between the Mn–B–Mn plane and the NH₂ group is somewhat larger than for the NMe₂ group. All the other geometry parameters are almost the same.

The changes in the geometries of the dimanganese cluster when CO is substituted by a BE ligand are small and very similar to those described earlier for the Fe₂(CO)₈ fragment. The most interesting observation is that the B–E bond lengths are all somewhat longer (0.02–0.03 Å) than in the [Fe₂(CO)₈–(BE)] systems, which indicates stronger π back-bonding in [Mn₂(Cp)₂(CO)₄–(BE)]. We conclude that there is evidence from the structural data for stronger electronic interaction, notably π back-bonding, with these binuclear metal carbonyl fragments than with the mononuclear ones.

Bond enthalpies and energy decomposition: We have verified this inference by considering the energy decomposition as given in Table 3 for the BE ligands at the bridging positions. The calculated bond energies show that in all cases the boron bond of the binuclear fragment is thermodynamically much more stable than the corresponding bond to bridging CO, and

the bonds are stronger for the dimanganese than for the diiron fragment. The differences between the BF, BNH₂, and BO⁻ ligands are minor, with the exception of the [Fe₂(CO)₈–(BO)]⁻ case where the bond is some 30 kcal mol⁻¹ stronger than for BF and BNH₂. Altogether the thermodynamic stability of these compounds is beyond doubt. We note that the dissociation energies are in the upper range of the values found for the mononuclear metal carbonyl fragments, but they certainly do not exceed the latter by very much. However, the $\Delta E^0 + \Delta E_{\text{prep}}$ term is much more destabilizing for the binuclear than for the mononuclear fragments. The comparable total dissociation energies thus imply that the electronic interactions are much stronger for the binuclear systems. This can indeed be verified in Table 3.

For the bridging AE ligands in [Fe₂(CO)₈–(AE)] the π bond is consistently stronger than in any mononuclear complex (up to twice as strong). A greater extent of π back-bonding to the bridging ligand is found for [Mn₂(Cp)₂(CO)₄–(AE)], some 30 kcal mol⁻¹ stronger than for the [Fe₂(CO)₈–(AE)] systems. A notable exception in both cases is BO⁻, which does show stronger π bonding than in the mononuclear complexes, and is stronger in [Mn₂(Cp)₂(CO)₄–(BO)]⁻ than in [Fe₂(CO)₈–(BO)]⁻ although the π bonding remains comparatively modest. The σ bonding is also quite strong in the binuclear systems, although not stronger than in the best σ acceptors among the mononuclear fragments Fe(CO)₄ and notably {Co(CO)₄}⁺. We have verified that the relatively strong π back-bonding has the expected effect of decreasing the positive charge at the B atom (i.e. the calculated Hirshfeld^[42] charges, Table 4).

We conclude that the binuclear fragments are ideally suited for stabilization of BE ligands, on three counts: 1) the [M₂–(BE)] complexes are thermodynamically quite stable; 2) there is steric protection by the large metal carbonyl fragment; 3) the strong π -bonding capability of the binuclear fragments will electronically stabilize the complexed ligand, by shifting the π -acceptor orbital with large amplitude on B to high energy and by reducing the positive charge on boron. In

fact the π^* orbitals of the ligands CO, BF, and BNH_2 make only a very small contribution (2–5%) to the LUMOs of the binuclear complexes compared with a contribution of 20–30% in the case of the mononuclear complexes.

Conclusions

BE molecules, coordinating through boron, can be viable ligands in the design of thermodynamically stable transition metal complexes. Problems associated with a possibly low kinetic stability may be solved through steric shielding and/or electronic stabilization of the reactive BE frontier orbitals. This follows from our density-functional theoretical study of the metal-binding capabilities of a series of isolobal ligands CO, BF, BO^- , BNH_2 , and $\text{BN}(\text{CH}_3)_2$ in mono- and binuclear first-row transition metal carbonyl complexes.

The high thermodynamic stability of the BE ligands has been traced to their being much better σ donors than CO, while they are (except for BO^-) comparable π acceptors. The reason is the much higher energy of the σ -donor orbital and comparable energy of the π^* orbital, the localization of these frontier orbitals at B and C being similar. On the other hand, the high polarity and small HOMO–LUMO gap of the (uncoordinated) BE ligand suggest a low kinetic stability. Of course, complexation increases the kinetic stability to a certain extent (by increasing the HOMO–LUMO gap), but the imbalance between σ donation and π acceptance leads to a build-up of positive charge on BE. In principle, this causes metal complexes of BE ligands, such as BF, to be rather sensitive towards nucleophilic attack.

The kinetic stability of BE complexes may be enhanced by steric protection of the BE ligand's reactive frontier orbitals. Such protection may be provided by bulky ligands in the metal complex or by complexation at a bridge site in a binuclear complex. BNR_2 can in addition provide its own steric protection with bulky R substituents, making it the most potentially useful ligand of the present series.

Another strategy for improving the kinetic stability may be to reduce the build-up of charge on the coordinated BE ligand by restoring the balance between M–BE σ donation and π back-donation. We have shown that binuclear metal complex fragments such as $\text{Fe}_2(\text{CO})_8$ and $\text{Mn}_2(\text{Cp})_2(\text{CO})_4$ have just the right frontier orbitals to do this. In particular, they have an excellent π -donor MO of the type $3d(\text{M}) - 3d(\text{M}')$, which is high in energy owing to metal–metal (π^*) as well as metal–ligand (e_g) antibonding interactions. This metal fragment orbital is an excellent π donor, which compensates for the fact that BF, BNH_2 and $\text{BN}(\text{CH}_3)_2$ are much better σ donors than π acceptors. This result suggests that the M–BE σ/π balance can be improved in mononuclear $[\text{M}(\text{CO})_n(\text{BE})]$ complexes too. One could replace CO molecules (which stabilize the metal $3d_\pi$) by ligands, which push the metal $3d_\pi$ orbital up in energy. This can be done, for example, with short-bridged biphosphino ligands, as has been shown by Hofmann.^[44]

The BO^- ligand differs substantially from the neutral boron ligands, although it is isolobal to them. This is of course as a result of the charge effect, which shifts the whole orbital spectrum upwards. BO^- is therefore an extraordinarily strong

σ donor and a very poor π acceptor. This ligand may well be used in conjunction with an oppositely charged metal fragment in order to synthesize a stable complex.

Acknowledgments: A.W.E., F.M.B and U.R. would like to thank the Deutsche Forschungsgemeinschaft (DFG) for postdoctoral fellowships. We thank the Netherlands Organization for Scientific Research (NCF/NWO) for providing a grant for supercomputer time.

Received: June 13, 1997 [F724]

- [1] J. P. Collman, *Acc. Chem. Res.* **1975**, *8*, 342.
- [2] K. H. Dötz, R. W. Hoffmann, *Organic Synthesis via Organometallics*, Springer, Berlin, **1991**.
- [3] C. Elschenbroich, A. Salzer, *Organometallics: A Concise Introduction*, VCH, Weinheim, **1992**.
- [4] F. M. Bickelhaupt, U. Radius, A. W. Ehlers, R. Hoffmann, E. J. Baerends, *New J. Chem.* **1998**, in press.
- [5] U. Radius, F. M. Bickelhaupt, A. W. Ehlers, N. Goldberg, R. Hoffmann, *Inorg. Chem.* **1998**, in press.
- [6] R. Criegee, G. Schroeder, *Justus Liebigs Ann. Chem.* **1959**, *623*, 1.
- [7] H. Nöth, *Angew. Chem.* **1988**, *100*, 1664; *Angew. Chem. Int. Ed. Engl.* **1988**, *27*, 1603.
- [8] T. B. Fehlner, D. W. Turner, *J. Am. Chem. Soc.* **1973**, *95*, 7175.
- [9] M. Groetklas, P. Paetzold, *Chem. Ber.* **1988**, *121*, 809.
- [10] H. Bock, L. S. Cederbaum, W. von Niessen, P. Paetzold, P. Rosmund, B. Solouki, *Angew. Chem.* **1989**, *101*, 77; *Angew. Chem. Int. Ed. Engl.* **1989**, *28*, 88.
- [11] R. Hoffmann, *Angew. Chem.* **1982**, *94*, 725; *Angew. Chem. Int. Ed. Engl.* **1982**, *21*, 711.
- [12] G. Schmid, W. Petz, H. Nöth, *Inorg. Chim. Acta* **1970**, *4*, 423.
- [13] H. Braunschweig, T. Wagner, *Angew. Chem.* **1995**, *107*, 904; *Angew. Chem. Int. Ed. Engl.* **1995**, *34*, 825; further details of the crystal structure investigations may be obtained from the Fachinformationszentrum Karlsruhe, 76344 Eggenstein-Leopoldshafen (Germany) on quoting the depository number CSD-401509.
- [14] A. Rosa, E. J. Baerends, *New J. Chem.* **1991**, *15*, 815.
- [15] E. J. Baerends, D. E. Ellis, P. Ros, *Chem. Phys.* **1973**, *2*, 41.
- [16] E. J. Baerends, P. Ros, *Chem. Phys.* **1973**, *2*, 52.
- [17] C. Fonseca Guerra, O. Visser, J. G. Snijders, G. te Velde, E. J. Baerends in *METECC-95* (Eds.: E. Clementi, C. Corongiu), Cagliari, **1995**, p. 307.
- [18] G. te Velde, E. J. Baerends, *J. Comp. Phys.* **1992**, *99*, 84.
- [19] J. G. Snijders, E. J. Baerends, P. Vernooijs, *At. Nucl. Data Tables* **1982**, *26*, 483.
- [20] P. Vernooijs, J. G. Snijders, E. J. Baerends, Internal report, Free University of Amsterdam (The Netherlands), **1981**.
- [21] J. Krijn, E. J. Baerends, Internal report, Free University of Amsterdam (The Netherlands), **1984**.
- [22] S. H. Vosko, L. Wilk, M. Nusair, *Can. J. Phys.* **1980**, *58*, 1200.
- [23] A. D. Becke, *Phys. Rev. A* **1988**, *38*, 3098.
- [24] J. P. Perdew, *Phys. Rev. B* **1986**, *33*, 8822.
- [25] L. Fan, L. Versluis, T. Ziegler, E. J. Baerends, W. Ravenek, *Int. J. Quantum Chem., Quantum Chem. Symp.* **1988**, *522*, 173.
- [26] L. Versluis, T. Ziegler, *J. Chem. Phys.* **1988**, *322*, 88.
- [27] L. Fan, T. Ziegler, *J. Phys. Chem.* **1992**, *96*, 6937.
- [28] C. von Wüllen, *J. Chem. Phys.* **1996**, *105*, 5484.
- [29] A. Rosa, A. W. Ehlers, E. J. Baerends, J. G. Snijders, G. te Velde, *J. Phys. Chem.* **1996**, *100*, 5690.
- [30] K. Morokuma, *Acc. Chem. Res.* **1977**, *10*, 244.
- [31] T. Ziegler, A. Rauk, *Inorg. Chem.* **1979**, *18*, 1755.
- [32] T. Ziegler, A. Rauk, *Theor. Chim. Acta* **1977**, *46*, 1.
- [33] F. M. Bickelhaupt, N. M. M. Nibbering, E. M. von Wezenbeek, E. J. Baerends, *J. Phys. Chem.* **1992**, *96*, 4864.
- [34] M. I. Bruce, *Chem. Rev.* **1991**, *91*, 197.
- [35] A. W. Ehlers, S. Dapprich, S. F. Vyboishchikov, G. Frenking, *Organometallics* **1996**, *15*, 105.
- [36] E. J. Baerends, A. Rozendaal, in *Quantum Chemistry: The Challenge of Transition Metals and Coordination Chemistry* (Eds.: A. Veillard, D. Reidel), Cordrecht, **1986**, p. 159.

- [37] T. Ziegler, V. Tschinke, C. Ursenbach, *J. Am. Chem. Soc.* **1987**, *109*, 4825.
- [38] A. W. Ehlers, G. Frenking, *J. Am. Chem. Soc.* **1994**, *116*, 1514.
- [39] a) G. Frenking, I. Antes, M. Böhme, S. Dapprich, A. W. Ehlers, M. Otto, R. Stegmann, A. Veldkamp, S. F. Vyboishchikov, in *Rev. Comput. Chem.*, Vol. 8 (Eds.: K. B. Lipkowitz, D. B. Boyd), VCH, New York, **1996**, p. 63; b) A. Ehlers, G. Frenking, *Organometallics* **1995**, *14*, 423.
- [40] J. Li, G. Schreckenbach, T. Ziegler, *J. Am. Chem. Soc.* **1995**, *117*, 486.
- [41] V. Jonas, W. Thiel, *J. Chem. Phys.* **1995**, *102*, 8475.
- [42] F. L. Hirshfeld, *Theor. Chim. Acta* **1977**, *44*, 129.
- [43] A. Cotton, J. M. Troup, *J. Chem. Soc. Dalton Trans.* **1974**, 800.
- [44] P. Hofmann, H. Heiss, G. Müller, *Z. Naturforsch.* **1987**, *B42*, 395.
-